Growth of the Huoerguosi anticline (north Tianshan Mountains) by limb rotation since the late Miocene

ShengLi WANG[1], Yan CHEN[2] and HuaFu LU[1]

Citation: Chinese Science Bulletin **53**, 3028 (2008); doi: 10.1007/s11434-008-0230-8

View online: https://engine.scichina.com/doi/10.1007/s11434-008-0230-8

View Table of Contents: https://engine.scichina.com/publisher/scp/journal/Sci Bull Chin/53/19

Published by the Science China Press

Chinese Science Bulletin

Growth of the Huoerguosi anticline (north Tianshan Mountains) by limb rotation since the late Miocene

WANG ShengLi[1†], CHEN Yan[2] & LU HuaFu[1]

[1] Department of Earth Sciences, Nanjing University, Nanjing 210093, China;
[2] Institut des Sciences de la Terre d'Orléans; Bâtiment Géosciences, rue de Saint Amand, BP 6759, 45067 Orléans Cedex 2, France

The Huoerguosi anticline, located in the north Tianshan Mountains piedmont fold-and-thrust belt, is a trending east-west fault-related fold. In the cross section along the Jingou River, its south limb is composed of the pre-growth strata of the Anjihaihe ($E_{2\text{-}3}a$), the Shawan ((E_3-N_1)*s*), the Taxihe (N_1t) and the lower part of the Dushanzi (N_2d) Formations, trending east-west and dipping to south 55°, and the growth strata of the upper part of the Dushanzi (N_2d) and Xiyu ((N_2-Q_1)*x*) Formations, dips of which decrease from 55° at the base of the growth strata to 47° at the bottom of the Xiyu ((N_2-Q_1)*x*) Formation to ~0° at the top of the Xiyu ((N_2-Q_1)*x*) Formation. The strata at the north limb of the anticline are vertical or over-turned, and are cut by the breakthrough thrusts to result in the drag fold. In the depth, the anticline is symmetric, and its core comprises the Cretaceous and the Jurassic coal-bearing beds. In the seismic profile, the seismic reflectors of pre-growth strata at the south limb of the anticline dip to south constantly, and ones of the growth strata fan southward, whose dips decrease upward. The geometry of the south limb growth strata outcropped along the Jingou River valley and the deep structure of the anticline shown in the seismic profile indicate that the Huoerguosi anticline is a detachment fold anticline growing by limb rotation. Based on the growth model and magnetostratigraphic age, during the growing process of the Huoerguosi anticline, the average shortening rate absorbed by the south limb is ~0.46 mm/a, and the average uplifting rate of the anticline is ~0.86 mm/a which exceeds the average deposition rate, which is in accordance with the fact that the top of the anticline is intensely eroded. Considering symmetric geometry of the Huoerguosi anticline and ignoring the breakthrough thrusts, the shortening of the whole anticline should be more than ~0.92 mm/a, doubling the shortening rate determined from the growth at the south limb.

Tianshan Mountains, Cenozoic, Huoerguosi anticline, limb rotation, growth strata

Cenozoic deformation of Eurasian interior is controlled by the India/Eurasia collision and consequent convergent tectonics[1]. The Tianshan Mountains are a Paleozoic orogen[2,3], and are reactivated by the India/Eurasia collision in the Early Miocene[4,5], which resulted in formation of the rejuvenation foreland basins in their bilateral piedmonts[4−6].

Meso-Cenozoic sedimentary strata were scraped off from the underlying blocks while the Tianshan Mountains thrust over the Junggar block[7], and propagated foreland to form the fold-and-thrust belt in the north Tianshan Mountains piedmont, which led to the crustal shortening in the interior of Eurasia. The crustal shortening in the fold-and-thrust belt can be identified quantitatively by researching on geometry and geochronology of growth strata[8]. Rivers in the north Tianshan Mountains piedmont widening and incision triggered by Pliocene climate change[9] shaped the U-type valley, about 100 m deep, even up to hundreds of meters at core of the anticline forming clear outcrop of structure and

Received December 26, 2007; accepted April 1, 2008; published online August 21, 2008
Doi: 10.1007/s11434-008-0230-8
†Corresponding author (email: wangsl@nju.edu.cn)
Supported by the National Natural Science Foundation of China (Grunt No. 40702031)

growth strata, such as at the valleys of the Manas, the Jingou, the Anjihai and the Kuitun River. All Cenozoic strata, including the Anjihaihe Formation ($E_{2\text{-}3}a$) and the above strata, crop out on the vertical cliffs of both sides of the Jingou River valley cutting across the Huoerguosi anticline perpendicularly. Magnetostratigraphic researches[10,11] constrain ages of upper Cenozoic strata accurately. This paper addresses the geometry and kinematics of the Huoerguosi anticline in the north Tianshan Mountains piedmont fold-and-thrust belt based on surface and seismic data along the Jingou River.

1 Geological setting

The north Tianshan Mountains piedmont fold-and-thrust belt, trending WNW to the west of Urumqi City, comprises three rows of anticline zones and the synclines between them, which are the Xihu-Dushanzi-Anjihai anticline zone as the north front, the Huoerguosi-Manas- Tugulu anticline zone in the middle, and the Qigu half-anticline zone. Deng et al.[12,13] deciphered the characteristics of the anticline zones and analyzed the formation ages of them. Lu et al.[14] reported the growth time and northward propagating vergence of the fold-and-thrust belt. The movement propagated from the north Tianshan Mountains piedmont fold-and-thrust belt is absorbed by folding and thrusting that cause great earthquakes[13,15−19] and deformation of the terraces[13,19−21] during the Quaternary.

The Huoerguosi anticline, located at the west segment of the second anticline zone, is linear in map view. The core of the anticline is composed of the Anjihaihe Formation ($E_{2\text{-}3}a$); the north limb of the anticline is composed of the Shawan ($(E_3\text{-}N_1)s$), the Taxihe (N_1t), the Dushanzi (N_2d) and the Xiyu ($(N_2\text{-}Q_1)x$) Formation, most of which are overturned to south and cut by breakthrough thrusts on surface; the south limb of the anticline comprises the Anjihaihe ($E_{2\text{-}3}a$), the Shawan ($(E_3\text{-}N_1)s$), the Taxihe (N_1t), the Dushanzi (N_2d) and the Xiyu ($(N_2\text{-}Q_1)x$) Formation, dipping in middle to shallow angles to south (Figure 1).

2 The structural features

The Huoerguosi anticline topographically exhibits a 300-m-high hill covered by sparse vegetation, and bedrocks crop out widely. The relative depth of the Jingou River valley is about 100 m at the syncline to the south of the anticline and up to 400 m at the middle part of the south limb of the Xiyu Formation ($(N_2\text{-}Q_1)x$) exposed in surface. The terraces at bilateral banks of the Jingou River are covered by Pleistocene or Holocene deposits with different thicknesses. The characteristics of the Huoerguosi anticline are exhibited along the Jingou River valley section (Figure 2). At the south limb of the anticline along the valley, the Anjihaihe ($E_{2\text{-}3}a$), the Shawan ($(E_3\text{-}N_1)s$), the Taxihe (N_1t) and the lower part of the Dushanzi (N_2d) Formation trend east-west, and dip to south 55° stably (Figure 2(a)). The striation of interlayers slips perpendicular to the strike of the bedding planes with constant occurrence are very common. The occurrence of the lower part of the Dushanzi Formation (N_2d) is in accordance with the underlying strata. But the dips of the upper part of the Dushanzi Formation (N_2d) decrease bed-by-bed from 55° at the middle part of the Dushanzi Formation (N_2d), to 46°, and to 30° at the top of the Dushanzi Formation (N_2d) (Figure 2(b)). There is not an abrupt lithology change between the Dushanzi (N_2d) and Xiyu Formations ($(N_2\text{-}Q_1)x$), but only a gradual transition exists, which is evidenced by

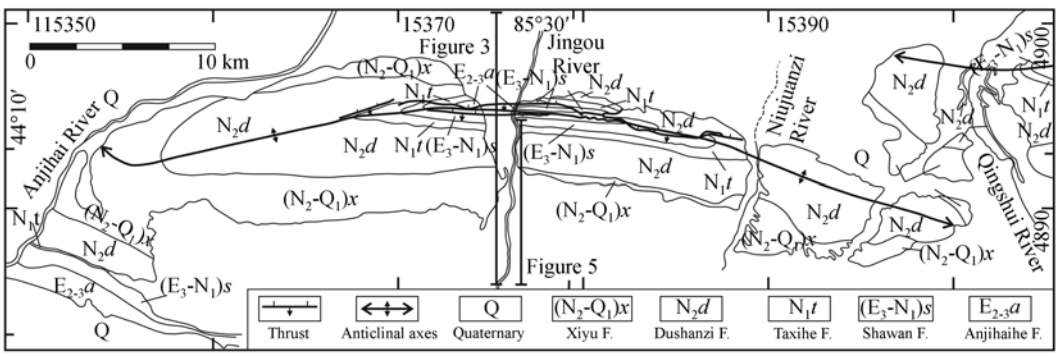

Figure 1 Geological map of the Huoerguosi anticline and adjacent area.

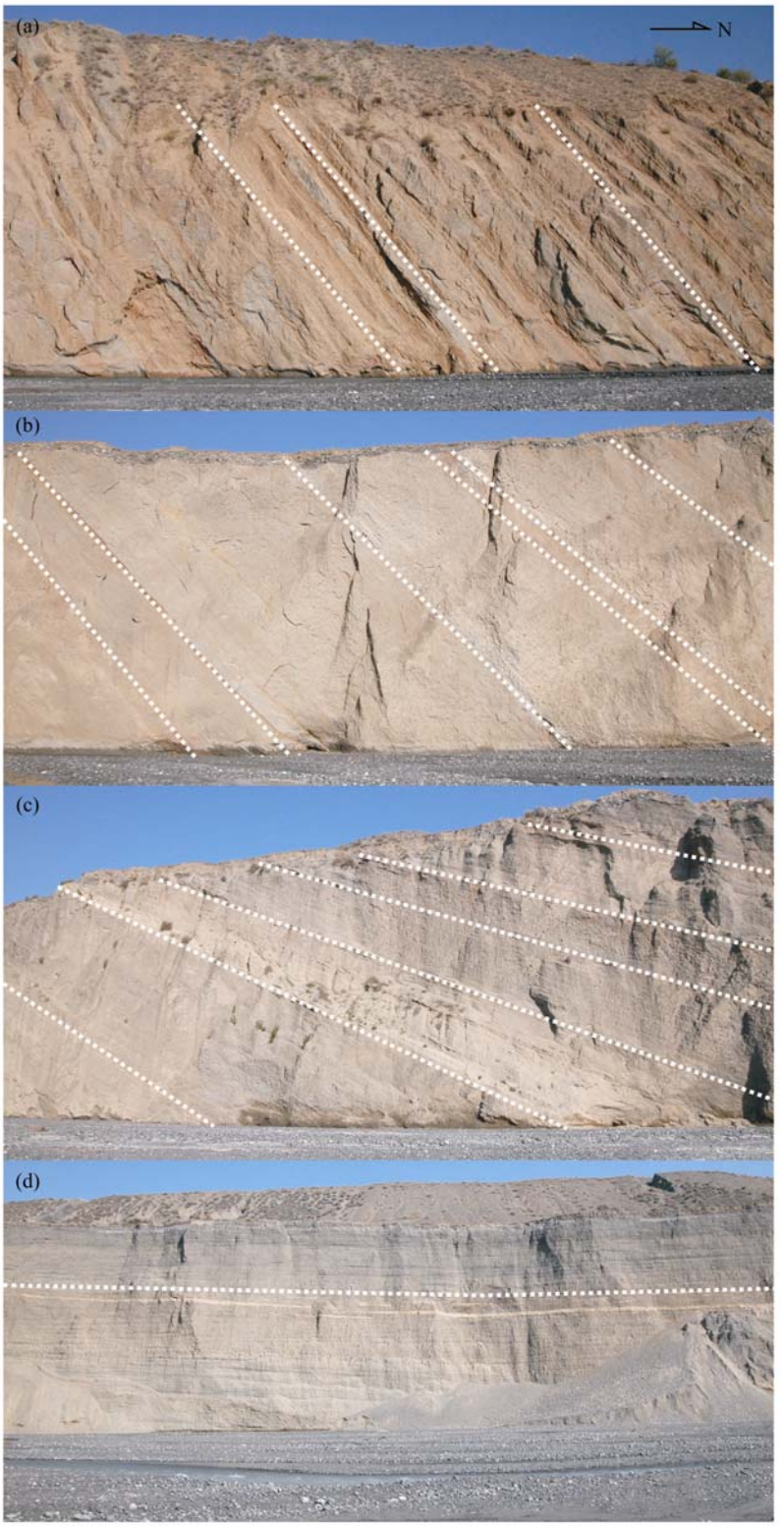

Figure 2 Photos of the growth strata at the south limb of the Huoerguosi anticline, taken along the Jingou River valley. (a) Looking west, but mirrored, and (b), (c) and (d) looking east. (a) Showing the north part of the south limb of the anticline, being pre-growth strata of the lower part of the Dushanzi Formation (N_2d) trending east-west, dipping to south 55° accordingly. (b) Showing the middle part of the south limb, being growth strata of the upper part of the Dushanzi Formation (N_2d) dipping to south from 45° to 38°. (c) Showing the middle part of the south limb, being growth strata of the middle part of the Xiyu Formation ((N_2-Q_1)x) dipping to south from 34° to 11°. (d) Showing the south end of the south limb, being growth strata of the Xiyu Formation ((N_2-Q_1)x), the horizontal beds of which onlap the underlying beds dipping to south gently.

the color variation of the strata from loess yellow of the Dushanzi Formation (N_2d) to gray as well as their conglomerate content (conglomerates of the Xiyu Formation ((N_2-Q_1)x) up to 80% in volume). The dips of the Xiyu Formation ((N_2-Q_1)x) decrease southward from 30° at the south limb to ~0° at the axial part of the syncline in the valley (Figure 2(d)). At the top of the Xiyu Formation ((N_2-Q_1)x), the horizontal strata onlap the underlying gently south dipping strata (Figure 2(d)). In the whole Jingou River section, the bedding planes of the upper part of the Dushanzi Formation (N_2d) and the Xiyu Formation ((N_2-Q_1)x) of the south limb of the anticline fan southward distinctly.

The seismic profile (Figure 3) reveals the subsurface structure of the Huoerguosi anticline. The north limb of the anticline, trending east-west and dipping to north no less than 80° or overturned gently, is noise area resulting in a non-reflector signal area in the seismic profile. The pre-growth strata at the south limb of the anticline display some parallel reflectors with constant dip in accordance with the outcrop. The conglomerates of the upper part of the Dushanzi (N_2d) and the Xiyu ((N_2-Q_1)x) Formation are noise area above 1.5 s in the seismic profile, because of deposits being cemented and stratified weakly and bad receiving condition for seismic receiver on the surface. Below 1.5 s, the dips of both limbs of the anticline are constant. At bilateral synclines of the anticline, the reflectors are continuous and undeformed, and there is no repetition, lack and deformation of the strata. The core of the anticline comprises some reflector assemblages similar to the reflectors of the horizontal Cretaceous and Jurassic coal beds at the synclines beside the anticline. The characteristics of the growth strata at the south limb of the anticline and of the core of it in the seismic profile implicate that the Huoerguosi anticline is a detachment fold anticline, detachment layer of which is the Jurassic coal beds.

3 Growing model

The south limb of the Huoerguosi anticline comprises the pre-growth strata including the lower part of the

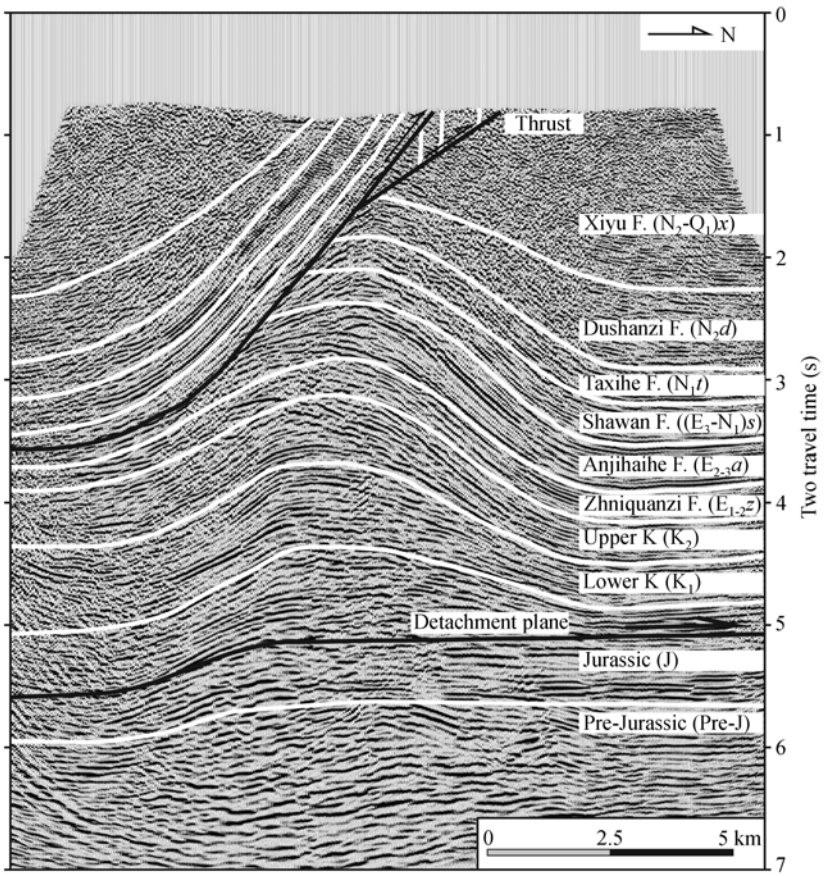

Figure 3 The interpreted seismic profile crossing the Huoerguosi anticline, for locations see Figure 1.

Dushanzi Formation (N_2d) and the underlying ones, and the growth strata of the upper part of the Dushanzi Formation (N_2d) and the Xiyu Formation ((N_2-Q_1)x), dips of which decrease southward, which is in accordance with the characteristics of the growth strata deposited at limb of detachment fold growing by limb rotation[22,23]. Buckling folding, fault-tip folding, displace gradient and trishear folding predict limb rotation during growing of fold[24], but the geometries of the controlling faults related with these folding are different from the fault below the detachment fold anticline. The fault-bend folding above the curved fault-bend can cause rotation of the limb, and dips of the growth strata above it decrease with their becoming young[25,26] and have characteristics of limb rotation. The seismic profile displays that Cretaceous and Jurassic coal-bearing strata make of the core of the Huoerguosi anticline and that the pre-growth strata above Jurassic strata are panel layers dipping south stably, which shows that fault-bend folding above curved fault-bend and shear fault-bend folding does not exist. All the above-mentioned show that the Huoerguosi anticline is a detachment fold anticline growing by rigid limb rotation of the south limb (Figure 4).

4 Construction of the south limb section

The breakthrough thrusts in the core of the Huoerguosi anticline cut the north limb of it and cause deformation of the bilateral terraces of the Jingou River[13,19−21]. Although the breakthrough thrusts extend about 22 km east-west, they do not change geometry of the anticline on the whole and the core of the anticline keeps intact, which indicates that reshaping of the anticline by them is weak. Therefore, we ignore the anticline's reshaping by the breakthrough thrusts while analyzing the geometry and kinematics of the Huoerguosi anticline. The hinge of the anticline crops out in the Jingou River valley, and the axial surfaces beside the hinge can determine width of the anticlinal crest and upper termination of the limbs. Based on the dip of the pre-growth strata measured along the walls of the Jingou River valley, and extrapolating the pre-growth strata to the axial surface beside the crest of the anticline, the interval between the anticlinal axial surface and the synclinal axial surface is width of the south limb. The growth strata are eroded partially during growing of the anticline. By extrapolating the growth strata in light of the dips of the growth strata, the growth strata would onlap the south limb of the anticline if the extrapolated growth strata onlap the strata under them. If the extrapolated growth strata reach the anticlinal axial surface, the growth strata would change abruptly their dips to become the crest of the anticline, but that does not exist in this case. To understand the geometry and kinematics of the Huoerguosi anticline adequately, we reconstruct the eroded strata in the south limb of the anticline with the technology mentioned above based on geometrical and kinematical characteristics of detachment folding[22,23].

Along the Jingou River valley, we observed and measured the occurrences of the strata bedded planes at the south limb of the Huoerguosi anticline, and located the coordinates of the measured pointes with portable GPS. The precision of the portable GPS location is 8 m, which satisfies the standard under which we research geometry and kinematics of the folding by analyzing the growth strata in thousands of meters scale. We reconstruct the geological section (Figure 5) of the south limb of the anticline with technology mentioned above based on the dips measured in the Jingou River valley and the deep geometry of the anticline showed on the seismic profile. The dips of the growth strata decrease with their becoming young in Figure 5, but the dips of six layers of them (gray layers in Figure 5) keep constant respectively, which shows that there are six times short quiescent intervals during the growing process of the anticline.

5 Growth and shortening determined from the growth strata at the south limb

The geometry of the Huoerguosi anticline is constrained

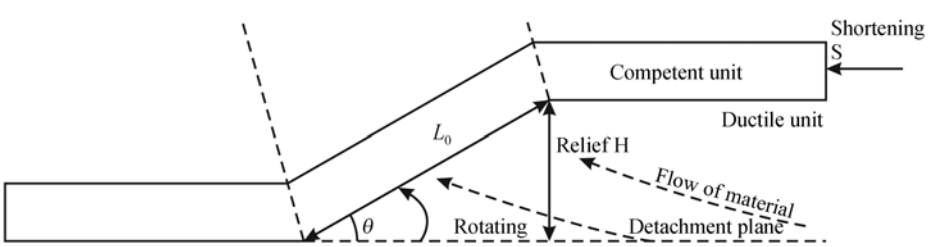

Figure 4 Geometrical model of progressive limb rotation[22].

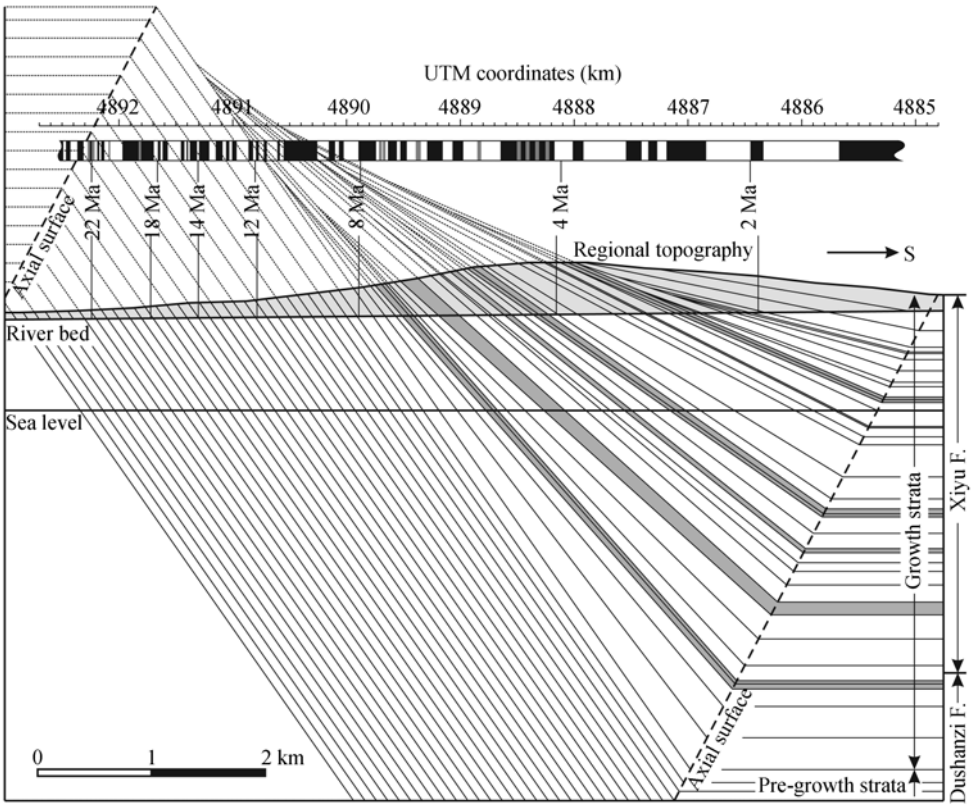

Figure 5 Geological section of the south limb of the Huoerguoss anticline, for locations see Figure 1. The regional topography is from the 1:100000 topographic map. The growth strata between the local topography and the Jingou River bed can be observed directly. The dashed lines represent the extrapolated pre-growth and growth strata bedded plane. The magnetostratigraphic column is from Charreau et al.'s work[1]. The thicknesses and the dips of gray intervals of the growth strata keep constant respectively.

by its south limb (Figure 5) based on the growth model and the occurrence data measured along the Jingou River valley. The shortening absorbed during development of the south limb is $S = L_0 \cdot (1-\cos\theta)$. The structural relief is $H = L_0 \cdot \sin\theta$. And the average shortening rate is $V=S/t = L_0 \cdot (1-\cos\theta)/t$. The instantaneous shortening velocity is $Vi = \mathrm{d}s/\mathrm{d}t = L_0 \cdot \sin\theta \cdot \mathrm{d}\theta/\mathrm{d}t$. Herein, S is the total shortening absorbed by development of the south limb during the growing process; L_0 is the width of the south limb; θ is the dip of the strata (Figure 4); and t is the age of corresponding layer of the growth strata. In Figure 5, the age of the base of the growth strata is ~8 Ma, the width of the south limb of the Huoerguosi anticline is ~8481 m, and the dip of the pre-growth strata is ~55°. Therefore, we conclude that the total shortening absorbed by the south limb rotation during the growing process is ~3490 m, and its total structural relief is ~6704 m.

We can induce the shortening and structural relief changing through time (Figures 6 and 7) determined from the growth strata based on the geometrical growth model of the Huoerguosi anticline, the dip and age of every growth strata layer (Figure 5). During the growing process of the anticline, the cumulative shortening and structural relief can be divided into two stages (Figures 6 and 7). In the first stage, 0—4 Ma B.P., the fitted linear functions of shortening (S) and uplifting (U) through time (t) are S_1=0.36t–0.26, and U_1=1.29t–0.24; the average shortening rate is ~0.36 mm/a and the average structural relief rate is ~1.29 mm/a. In the second stage, 4—8 Ma B.P., they are S_2=0.58t–1.14 and U_2=0.6t + 2.0; the average shortening rate is ~0.58 mm/a and the average structural relief rate is ~0.6 mm/a. During the whole growth of the anticline, 0—8 Ma B.P., they are S=0.46t–0.45, and U=0.86t+0.58; the total average shortening and uplifting velocities are ~0.46 mm/a and ~0.68 mm/a

1) Charreau J, Avouac J P, Chen Y, et al. Miocene to present kinematics of folding and thrusting across Huoerguosi anticline, North Tianshan (China), 2007, submitted.

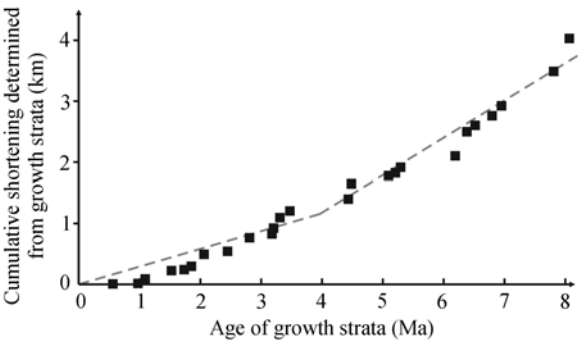

Figure 6 The relationship between the shortening of the Huoerguosi anticline and time determined from the growth strata. The shortening during the growing process of the anticline increases through time.

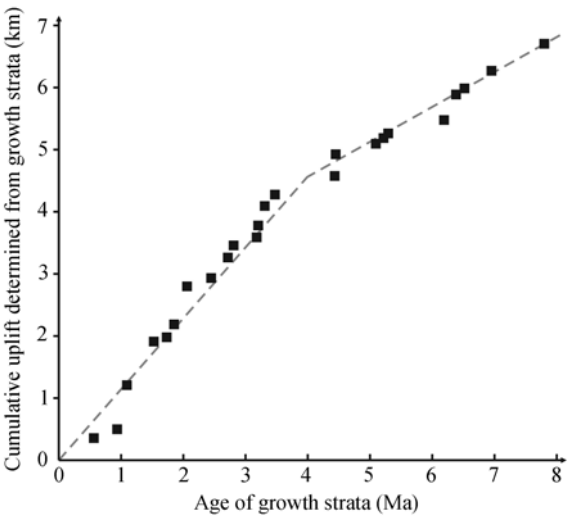

Figure 7 The relationship between the structural relief of the Huoerguosi anticline and time determined from the growth strata.

respectively.

6 Discussion and conclusions

The Huoerguosi anticline had been looked as constant thickness fault-propagation fold, and durative propagation of the fault ramp broke through its north limb to cause deformation of the terraces across the anticline[13,14,18,19]. The constant thickness fault-propagation fold grows by kink-band migration[24,27] to form growth triangles above frontal and back limbs[8], which are different from the phenomenon observed in the Jingou River section. Moreover, the deformation of the terraces of the Jingou Rive is buckling[13,19,20], which is different from constant thickness fault-propagation folding by kink-band migration, but is in accordance with detachment folding by limb rotation. Some workers thought that the Huoerguosi anticline began to grow in the Early Pleistocene based on the angular unconformity between the Middle Pleistocene and the underlying Tertiary or the Lower Pleistocene[13,18,19]. During the fold growing process, change of ratio between structural relief and deposition rate or local erosion can cause angular unconformity at crest or limb[8,22,24]. Local angular unconformity does not represent initiation or termination of folding, but whole architecture of growth strata is one reliable marker for determining fold growing process[8].

The growth strata show that during the growing process of the Huoerguosi anticline the crustal shortening absorbed by the south limb of the anticline is ~3490 m and the average shortening rate is ~0.46 mm/a. Taking the approximate symmetric geometry of the Huoerguosi anticline in the deep into account, the total shortening of the anticline should be double times of the south limb. Due to our overlook to effect of the breakthrough thrusts, the total shortening of the anticline should be no less than ~0.92 mm/a. The changing of the shortening and uplifting velocities of the Huoerguosi anticline may be occurred temporarily during relative constant development of the fold-and-thrust belt[28]. Due to different understanding of the folding mechanism of the Huoerguosi anticline, our shortening and uplifting velocities are different from the data given by Feng et al.[18]. Because of different cognition of the thrusting and folding initiation age and different working areas, our results do not agree with Burchfiel et al.'s work[29] on east and west segments of the north Tianshan Mountains, and are less than the shortening of 3±1.5 mm/a[21] gotten by measuring deformation of the Manas River terraces.

The total relief of the Huoerguosi anticline is ~6704 m, which does not occur as the current relative height because part of it is covered by the growth strata. The uplifted strata were eroded intensely, which causes the relative height of about 400 m located at the conglomerates of the Xiyu Formation ($(N_2\text{-}Q_1)x$) that have strong weatherproof capacity. The average uplifting velocity of ~0.86 mm/a is approximately equivalent to the vertical uplift rate determined from deformation of the terraces[13,19−21]. The average uplifting rate is obviously more than the deposition rate in this area and 0.21±0.01 mm/a in the Kuitun River area since 10 Ma[11], which is in accordance with the fact that the pre-growth and growth strata above the local plane of denudation were eroded intensely. The distinct changing of the shortening and uplifting velocities at about 4 Ma B.P. coincides

with global climate change at 2—4 Ma[30]. Maybe, the erosion velocity increase resulting from the global climate change[30] causes the changing of the uplifting and shortening of the Huoerguosi anticline.

The GPS measurements[31—33] showed the crustal shortening in the Tianshan Mountains region. Niu et al.[33] reported that the crustal shortening velocities in the Tianshan Mountains region decreased from the west to the east segment, and the average crustal shortening was 12 mm/a equivalent to the shortening at the middle segment of the Tianshan Mountains. These are the whole image of active tectonics in the south and north piedmonts and the interior of the Tianshan Mountains in decade scale. The average shortening rate in millions of years scale during the growing of the Huoerguosi anticline determined from the growth strata at its south limb is an image of single structures, and is only one component of the whole Tianshan Mountains deformation, therefore it is different from GPS measurements.

There exist six beds with constant dips in the growth strata which show that there exists the short-term structural quiescence during growing of the anticline. This phenomenon is being in folding caused by blind thrust[34]. The temporal quiescence could be related to the process that when the north Tianshan Mountains fold-and-thrust belt propagates to foreland to develop a new row of anticline it forms the stable critical taper with the Huoerguosi anticline uplifting. In fact, the Anjihai anticline to the north of the Huoerguosi anticline began to grow at that age[35]. Due to the decreasing of the height of the anticline caused by erosion, the Huoerguosi anticline continues to develop.

The Huoerguosi anticline is a growing anticline located in the north Tianshan Mountains piedmont fold-and-thrust belt. The dips of the growth strata comprising the upper part of the Dushanzi (N_2d) and the Xiyu Formation ((N_2-Q_1)x) decrease with their becoming young to fan southward. Taking the deep geometry exhibited in the seismic profile into account, we conclude that the Huoerguosi anticline is a detachment fold anticline growing by rigid limb rotation. Its north limb is cut by the breakthrough thrusts in the later stage. The shortening rate of the anticline during the total growing process determined from the growth strata is no less than 0.92 mm/a.

We thank Prof. Chen Jie and an anonymous reviewer for their thoughtful reviews, which greatly improved this manuscript.

1 Tapponnier P, Molnar P. Active faulting and Cenozoic tectonics of the Tien Shan, Mongolia and Baykal regions. J Geophys Res, 1979, 84: 3425—3459

2 Windley B F, Allen M B, Zhang C, et al. Paleozoic accretion and Cenozoic redeformation of the Chinese Tien Shan range, central Asia. Geology, 1990, 18: 128—131[DOI]

3 Chen C, Lu H, Jia D, et al. Closing history of the southern Tianshan oceanic basin, western China: an oblique collisional orogeny. Tectonophysics, 1999, 302: 23—40[DOI]

4 Lu H, David G H, Jia D, et al. Rejuvenation of the Kuqa foreland basin, north flank of the Tarim basin, northwest China. Int Geol Rev, 1994, 36: 1151—1158

5 Sobel E R, Dumitru T A. Thrusting and exhumation around the margins of the western Tarim Basin during the India-Asia collision. J Geophys Res, B, Solid Earth and Planets, 1997, 102(3): 5043—5063[DOI]

6 Liu H F. Classification of foreland basins and fold thrust style. Earth Sci Front (in Chinese), 1995, 2(3-4): 59—68

7 Zhao J, Liu G, Lu Z, et al. Lithospheric structure and dynamic processes of the Tianshan orogenic belt and the Junggar basin. Tectonophysics, 2003, 376: 199—239[DOI]

8 Suppe J, Chou G T, Hook S C. Rates of folding and faulting determined from growth strata. In: McClay K R. ed. Thrust Tectonics. New York: Chapman and Hall, 1992. 105—121

9 Molnar P, Brown E T, Burchfiel B C, et al. Quaternary climate change and the formation of river terraces across growing anticlines on the north flank of the Tien-Shan, China. J Geol, 1994, 102: 583—602

10 Sun J, Zhu R, Bowler J. Timing of the Tianshan Mountains uplift constrained by magnetostratigraphic analysis of molasse deposits. Earth Planet Sci Lett, 2004, 219: 239—253[DOI]

11 Charreau J, Chen Y, Gilder S, et al. Magnetostratigraphy and rock magnetism of the Neogene Kuitun He section (northwest China): implications for Late Cenozoic uplift of the Tianshan Mountains. Earth Planet Sci Lett, 2005, 230: 177—192[DOI]

12 Deng Q D, Feng X Y, Zhang P Z, et al. Reverse fault and fold zone in Urumqi rang-front depression and its genetic mechanism. Earth Sci Front (in Chinese), 1999, 6(4): 191—201

13 Deng Q D, Feng X Y, Zhang P Z, et al. Active Tectonics of Chinese Tianshan Mountains (in Chinese). Beijing: Seismological Press, 2000. 399

14 Lu H F, Wang S L, Jia C Z. The mechanics of the southern Junggar Cenozoic thrust. Earth Sci Front, 2007, 14(4): 168—174[DOI]

15 Yang X P, Deng Q D, Zhang P Z, et al. Active reverse fault-fold zones and estimation of potential earthquake source in northern Tianshan. Seismol Geol (in Chinese), 1998, 20(3): 193—200

16 Zhang P Z, Deng Q D, Xu X W, et al. Blind thrust, folding earthquake, and the 1906 Manas earthquake, Xinjiang. Seismol Geol (in Chinese), 1994, 16(3): 193—204

17 Feng X Y, Chen J, Li J, et al. Preliminary research of paleo-earthquake along the Huoerguosi fault zone. In: Deng Q D, ed. Research on Active Faults (2) (in Chinese). Beijing: Seismological

Press, 1992. 95－104
18 Feng X Y, Chen J, Li J, et al. The fault-propagation folding of the Huoerguosi active structure. Inland Earthquake (in Chinese), 1993, 7(4): 335－343
19 Li J, Feng X Y, Chen J, et al. Activity of the Huoerguosi active fold and thrust fault zone. In: Deng Q D, ed. Research on Active Faults (2) (in Chinese). Beijing: Seismological Press, 1992. 105－116
20 Xu X W, Deng Q D, Zhang P Z, et al. Deformation of river terrace across the Manas-Huoerguosi reverse fault and fold zone ant its neotectonics implication in Xinjiang. In: Deng Q D, ed. Research on Active Faults (2) (in Chinese). Beijing: Seismological Press, 1992. 18－32
21 Avouac J P, Tapponnier P, Bai M, et al. Active thrusting and folding along the northern Tien-Shan and late Cenozoic rotation of the Tarim relative to Dzungaria and Kazakhstan. J Geophys Res-Solid Earth, 1993, 98: 6755－6804[DOI]
22 Hardy S, Poblet J. Geometric and numerical model of progressive limb rotation in detachment folds. Geology, 1994, 22: 371－374[DOI]
23 Poblet J, McClay K. Geometry and kinematics of single layer detachment folds. Am Assoc Petrol Geol Bull, 1996, 80(7): 1085－1109
24 Suppe J, Sabat F, Munoz J A, et al. Bed-by-bed fold growth by kind-band migration: Sant Lorence de Morunys, eastern Pyreness. J Struct Geol, 1997, 19(3-4): 443－461[DOI]
25 Xiao H, Suppe J. Origin of rollover. Am Assoc Petrol Geol Bull, 1992, 76: 509－525
26 Medwedeff D W, Suppe J. Multibend fault-bend folding. J Struct Geol, 1997, 19(3-4): 279－292[DOI]
27 Suppe J, Medwedeff D A. Geometry and kinematics of fault-propagation folding. Eclogae Geol Helv, 1990, 83(3): 409－454
28 Davis D, Suppe J, Dahlen F A. Mechanics of fold-and-thrust belts and accretionary wedges. J Geophys Res, 1983, 88 (B2): 1153－1172[DOI]
29 Burchfiel B C, Brown E T, Deng Q D, et al. Crustal shortening on the margins of the Tien Shan, Xinjiang, China. Int Geol Rev, 1999, 41: 665－700
30 Zhang P, Molnar P, Downs W. Increased sedimentation rates and grain sizes 2－4 Myr ago due to the influence of climate change on erosion rates. Nature, 2001, 410: 891－897[DOI]
31 Abdrakhmatov K Y, Aldazhanov S A, Hager B H, et al. Relatively recent construction of the Tien Shan inferred from GPS measurements of present-day crustal deformation rates. Nature, 1996, 384: 450－453[DOI]
32 Reigber C, Michel G W, Galas R, et al. New space geodetic constraints on the distribution of deformation in central Asia. Earth Planet Sci Lett, 2001, 191: 157－165[DOI]
33 Niu Z J, You X Y, Yang S M. Analysis of contemporary crustal deformation characteristics with GPS data of Tianshan Mountain. J Geod Geodyn (in Chinese), 2007, 27(2): 1－9
34 Dolan J F, Christofferson S A, Shaw J H. Recognition of paleoearthquakes on the Puente Hills blind thrust fault, California. Science, 2003, 300: 115－118[DOI]
35 Daëron M, Avouac J-P, Charreau J. Modeling the shortening history of a fault tip fold using structural and geomorphic records of deformation. J Geophys Res, 2007, 112: B03S13, doi: 10.1029/2006JB004460[DOI]